Tribol Lett (2010) 37:273–281
DOI 10.1007/s11249-009-9521-8

ORIGINAL PAPER

Measurement of Friction Noise Versus Contact Area of Rough Surfaces Weakly Loaded

Alain Le Bot · E. Bou Chakra

Received: 15 May 2009 / Accepted: 14 September 2009 / Published online: 24 September 2009

Abstract This study presents an experiment to measure the dependence of friction noise versus the nominal contact area. The friction-induced vibration is generated by the sliding of two rough surfaces. The normal load is low leading to a weak contact. The normal load and the sliding velocity are maintained constant. The nominal contact area ranges over two orders of magnitude. It is found that two regimes exist. On the one hand, the vibration energy is proportional to the contact area. But on the second hand, the vibration energy is constant, i.e., does not depend on the contact area.

Keywords Surface roughness · Friction sound · Energy conservation · Friction mechanism · Stick-slip

1 Introduction

Friction noise appears in many industrial and natural systems. Squealing of breaks, squeaking of doors, tyre-road rolling noise, and cracking of joints are some examples of man-made systems where the noise can be a real nuisance and for which many efforts have been made to reduce them. In contrast, musical instruments such as violin and insect noises such as cricket and locust are some examples where friction noise is a desirable phenomenon.

A. Le Bot (✉) · E. Bou Chakra
Laboratoire de tribologie et dynamique des systèmes CNRS, Ecole centrale de Lyon 36 Avenue, Guy de Collongue, Ecully 69134, France
e-mail: alain.le-bot@ec-lyon.fr

E. Bou Chakra
e-mail: elie.bou-chakra@ec-lyon.fr

According to Akay [1], friction noises can be classified in two types depending on the contact pressure. When the contact pressure is high, the contact is strong. The friction noise originates from mechanical instabilities into the contact such as stick-slip [2]. The sound is produced by the vibrational response of the coupled solids. The sound pressure level is high and the sound is confined into a narrow frequency band. But when the contact is weak, the interface is made up of two rough surfaces whose asperity summits hit each other. The resulting noise is rather low and the frequency band is broad. This kind of friction noise is often called roughness noise meaning that the surface roughness is responsible of normal vibration.

In this article, the term roughness noise is used to refer to the particular kind of friction noise generated by the rubbing of rough surfaces under light loading without any apparent stick-slip. In these conditions, the underling mechanism which generates the sound is the normal vibration of surfaces induced by shocks between antagonist asperities. The frequency band of this friction-induced vibration is wide and the resulting noise is close to a white noise.

The normal vibration induced by the sliding contact of rough surfaces have been studied for several decades [3–5]. The key phenomenon responsible of vibration is the Hertzian normal contact submitted to a random excitation [6].

In addition to these fundamental studies, several experiments have been conducted on friction noise induced by normal vibration. They clarify the dependence of roughness noise with roughness and sliding speed. Othman et al. [7, 8] studied the contact between a stylus and a rough surface, Yokoi and Nakai [9] did the experiment with a rod–disk contact and the plane–plane contact has been tackled by Kato et al. [10], Stoimenov et al. [11], and

Ben Abdelounis et al. [12]. Although all these experimental setups are quite different and therefore several sliding regimes are covered, it seems that there is an agreement around a power law,

$$P_a \propto Ra^{\alpha} V^{\beta} \tag{1}$$

where P_a is the radiated acoustic power that is the total acoustic power being radiated by the vibrating surface, Ra the arithmetic roughness of the surface (some authors used different roughness criteria but the conclusion is similar), and V the sliding velocity.

The question which now arises is whether it is possible to generalize this relationship to the dependence with the contact area. Since the friction sound is produced in the friction zone, it could be guessed that a larger friction zone produces a strongest sound. If S denotes the apparent contact area between the two solids, a generalization of Eq. 1 could be,

$$P_a \propto Ra^{\alpha} V^{\beta} S^{\lambda/10} \tag{2}$$

Chosen in this way, the exponent λ is expressed in dB/decade. The underlying question is whether the sound power P_a is proportional to the apparent contact area S or in other words, if $\lambda = 10$.

The distinction between actual and apparent contact area is indeed very important for all questions related to contact problems. The apparent area of contact (or nominal contact area) can easily be controlled in an experiment. But it is well-known in tribology that friction is rather controlled by the actual contact surface. Measurement of actual contact area usually requires quite elaborated apparatus [13, 14]. As a preliminary discussion, this study focuses on the dependence of roughness noise with contact area in case where there is a proportionality between apparent and actual contact area. For this purpose, the contact is split into n similar contact zones, each of them being an independent sliding solid. All sliding solids have a same nominal contact area S_0 and a same actual contact area. The total apparent contact area is therefore $S = nS_0$ which, in turn, is proportional to the actual contact area. The question is therefore to measure the law of roughness noise versus the number n of sliding solids.

It is well-known in acoustics that if n similar acoustic sources are uncorrelated, their powers are additive and the sound pressure level is increased by 10 dB per decade of n. And n independent sliding solids can be considered as uncorrelated. Therefore, it could be guessed that the vibrational level induced by friction is simply proportional to the number n of sliding solids that is $\lambda = 10$. But, it is not clear from the literature that this linear law is valid.

This article presents the results of an experimental study on the dependence of roughness noise with the number n of sliding solids. In particular, the question of the validity of Eq. 2 is discussed.

2 Experimental Setup

Three objects are involved to produce the friction sound: Two solids, one being sliding and one being vibrating, and a surface. The slider contains the kinetic energy. The surface by which the interaction process occurs, transfers the kinetic energy onto vibrational energy. And the resonator is the solid where vibrational waves propagate. Finally, the sound is radiated into the air.

The last step is well-known [15]. The radiated acoustic power P_a is proportional to the square of the vibrational velocity. More exactly, if $v(\mathbf{x}, t)$ denotes the vibrational velocity at point $\mathbf{x}$ and time t in steady-state condition, the RMS-vibrational velocity is given by,

$$v(\mathbf{x}) = \sqrt{\frac{1}{\Delta T}\int_{\Delta T} v(\mathbf{x}, t)^2 dt} \tag{3}$$

where ΔT is the time window where the signal is acquired. The radiated acoustic power P_a is then proportional to the squared RMS-vibrational velocity v integrated over the radiating surface A, that is,

$$P_a = \rho_0 c \sigma \int v^2 dA \tag{4}$$

where ρ_0 is the density of air, c the sound speed and σ the so-called radiation factor. Another way to express this relationship is that the radiated acoustic power is proportional to the vibrational energy,

$$P_a \propto \int W dA \tag{5}$$

where $W = mv^2$ is the vibrational energy density, m being the mass per unit area of the plate. The RMS-vibrational velocity v is therefore the quantity that must be measured at all points to assess the radiated acoustic power P_a and consequently, the sound pressure level.

This experiment is based on a clear separation of the three functions, slider, surface and resonator. Several rigid solids, the sliders, are pulled on a thin rectangular plate, the resonator. The principle of the experiment is to measure the evolution of the RMS-vibrational velocity v versus the number of sliders n while the sliding velocity V is maintained constant.

The experimental setup is shown in Fig. 1. A brushless servomotor (type Danaher AKM22C) pulls the sliders with a string. The string is fixed to the pulley (radius 14 mm) of the motor in its first end and to the sliders at the second end. The sliding velocity V of the motor is measured by a

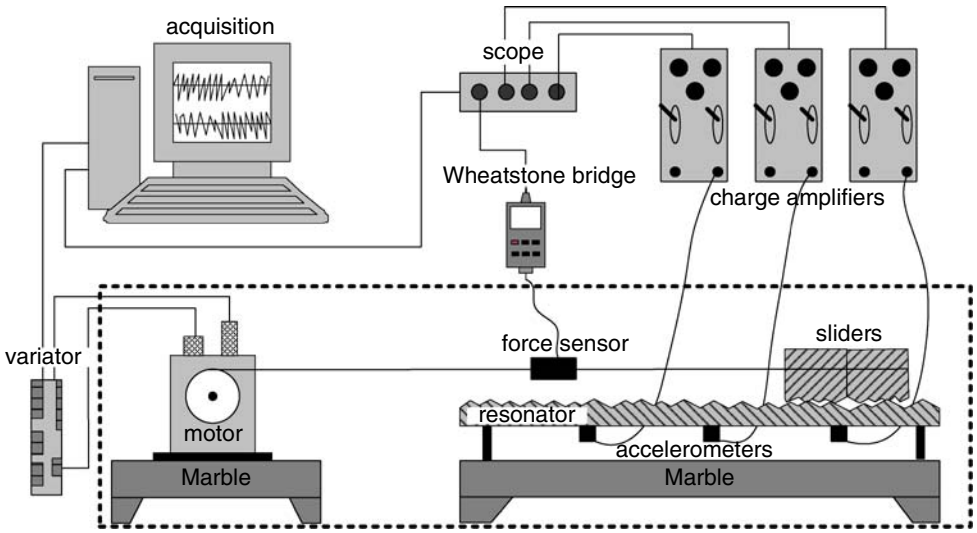

Fig. 1 Experimental setup. The sliders are pulled on the resonator by a servomotor. The sliding velocity V is maintained constant. The sliding on the rough track induces vibration v measured by three accelerometers. The friction force T is measured on the thread by a force sensor

decoder. It is maintained constant by a feedback loop with electrical variator (Servostar 300). The accuracy of the velocity is 1%. The traction force T is measured by a gauge force sensor (resolution of 0.001 N) placed in the string between the motor and the sliders. The RMS-vibrational velocity v is measured within the frequency band [10 Hz–10 kHz] at three points by three piezo-electric accelerometers (type B & K 4393 V sensibility 0.3 pC/ms^{-2}) and their charge amplifiers (type B & K 2635). The signal is acquired by a 16 bits A/D board with a sampling frequency 40 kHz. The acquisition time ΔT is approximately 2 s during the stable phase of the sliding velocity.

The sliders are parallelepipedic solids made of stainless steel. They have dimension 20 × 20 × 10 and 20 × 20 × 20 mm. Their first eigenfrequencies are computed by finite element method with density $\rho = 7{,}800$ kg/m^3, Young modulus $E = 210$ Gpa, and Poisson's ratio $v = 0.3$. They are respectively 50 and 70 kHz (Table 1). These natural frequencies are largely beyond 10 kHz and therefore the sliders can be considered as being infinitely rigid.

The resonator is a plate also made of stainless steel. Two dimensions of rectangular plates have been used 200 × 300 × 2 and 300 × 450 × 2 mm. A damping material layer can be stuck on the back side of plates in order to increase their internal damping. The plates used in the experiments are referenced by capital letters A, B, and C. Plate A has dimension 200 × 300 × 2 mm and a damping layer is stuck, plate B has same dimensions but without damping material and plate C has dimension 300 × 450 × 2 mm with a damping layer. The internal damping of vibrating structures is usually introduced with the so-called damping loss factor η in the following way. If all modes are located within a frequency band centred on ω (rad/s) then the vibrational power density being dissipated is $p_{\text{diss}} = \eta\omega W$ where W is the vibrational energy density. Basically, the separate values of η and ω can be measured with a modal analysis of the system. But a direct way to assess their product is to measure the impulse response $h(t)$ of the system. The time-decreasing of the impulse response results from all modes simultaneously excited. By examining the Schroeder's plot defined as the time-reversed integration,

$$t \mapsto \int_t^\infty h^2(\tau)\mathrm{d}\tau \tag{6}$$

it is possible to determine the reverberation-time T_r (the time for a decay of 60 dB of the vibrational impulse response). The product $\eta\omega$ then follows from $\eta\omega = 2\pi \times 2.2/T_r$. Values of T_r and $\eta\omega$ are shown in Table 2.

The resonators have been chosen to contain many modes within the frequency range of measurement (up to 10 kHz). The resulting vibrational field is diffuse, that is homogeneous and isotropic. The general conditions which lead to a diffuse vibrational field in rectangular plates

Table 1 Properties of sliders

Slider	Thin	Thick
Width × length × thickness (mm)	20 × 20 × 10	20 × 20 × 20
Mass M (g)	31.3	62.8
First natural frequency (kHz)	50	70

The first natural frequencies are large compared with the upper frequency of measurement 10 kHz.The sliders can be considered as rigid bodies

Table 2 Properties of resonators

Resonator	A	B	C
Width × length × thickness (mm)	200 × 300 × 2	200 × 300 × 2	300 × 450 × 2
Mass M (kg)	1.2	0.9	2.9
Reverberation time T_r (s)	0.4	21	0.3
Internal damping $\eta\omega$ (rad/s)	34	0.6	46
Number of modes N	95	95	215

The number of modes N is large meaning that the vibrational field is diffuse

have been studied in [16, 17]. It has been shown that the mode count that is the number of modes within the frequency range of interest is the most important criterion. This state of diffuse field can arise even when waves specularly reflect on boundaries [18, 19]. When the field is diffuse, the vibration is the same at any time during the sliding and so, can be considered as stationary. This is indeed important for the experiment to measure the vibration in stationary conditions. Another advantage to use diffuse field is that the exact position of the accelerometer measuring the vibration is of no importance.

The base of sliders and the track on the resonator are prepared by grinding. Two types of particles are blasted on the surfaces. The first type is brown corundum grits whose particles have a size about 1 mm. The resulting surfaces have a roughness about $Ra = 5\mu m$. The second type is glass beads with a size about 300μm. The resulting surfaces have a roughness about $Ra = 1\mu m$. Other roughness parameters of standard ISO4287 are summarized in Table 3. The roughness of the sliding surface is the same on both the resonator and the base of sliders. The surface topography is random, homogeneous and isotropic. Furthermore, the values of the skewness and the kurtosis highlight that the distribution of heights is almost Gaussian (RSk = 0 and RKu = 3 for a perfect Gaussian distribution).

The resonator is fixed on a heavy marble with four screws at corners. The servomotor is fixed on a second marble which is isolated from the first marble in order to reduce the transmission of vibration between the servomotor and the resonator. The two marbles, the servomotor, the resonator and the sliders are placed into a laminar flow hood to maintain air contaminants outside the working area. Thus, the quality of air is maintained constant as pure as possible. Temperature and moisture are measured during the experiment.

Table 3 Properties of surfaces

Surface	Corrindum grits	Glass beads
Grain size (μm)	1000	300
Arithmetic roughness Ra (μm)	5.0 ± 0.3	1.3 ± 0.1
Quadratic roughness Rq (μm)	6.3 ± 0.3	1.6 ± 0.1
Skewness RSk	− 0.3 ± 0.3	0 ± 0.2
Kurtosis RKu	3.1 ± 0.2	2.7 ± 0.3
RSm (μm)	245 ± 30	240 ± 40

Mean values and the standard deviations of measurements at six locations and in six directions of the surfaces. The roughness parameters are defined in the standard ISO4287

3 Protocol

The experimental protocol is the following. Just after the rough surfaces are prepared by grinding, the wear is rapid. To break the sharp angles of the rough profiles, a running period is necessary. Thus, the experiments have been conducted after a running period of about 25 shots. All sliders were used during the running period and the track on the resonator was entirely covered by the sliders in order to have a homogeneous wear. After this running period, it has been observed that the repetitivity of measurements is acceptable over several dozens of shots (the number of shots required by a typical experiment). It means that wear of surfaces induced by these following shots does not significantly affect the RMS-vibrational velocity.

The cleaning of the surfaces is one of the most important step in order to obtain an acceptable repetitivity of the experiment. The surfaces are cleaned several times during the experiment. Each cleaning is first done with heptane to remove all greases and secondly with propanol for residual traces. The surface is finally dried under a flux of nitrogen.

The sliders are carefully handled by the experimenter who uses latex gloves under the laminar flow hood with controlled temperature and moisture. The impulse response of the resonator is measured after its mounting on the marble, with four different points of excitation and with an oscilloscope and a microphone. One hundred sliders have been used in the experiment. In order to ensure a similar wear on all sliders, they are positioned in a queue and are used in this order. In this way, all sliders are used the same number of times. In addition, they are turned of 90 degrees after each sliding. To compare the results each series of experiment must be realized under same condition of temperature and moisture.

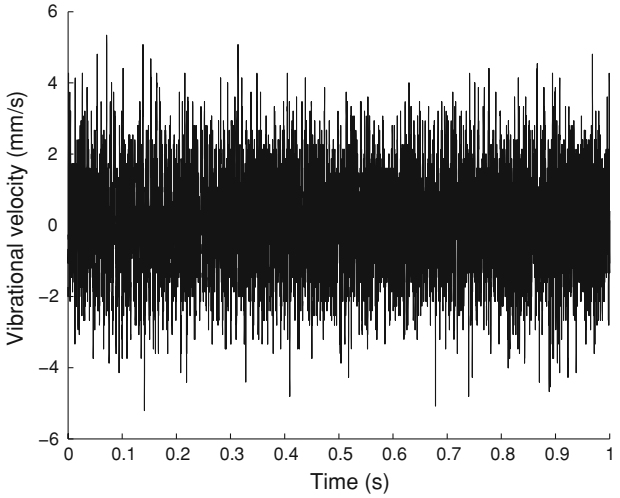

Fig. 2 Example of roughness noise. Vibrational velocity versus time measured by accelerometer

4 Experimental Results

In Fig. 2 is shown an example of time-evolution of vibrational velocity measured by an accelerometer. This signal, acquired with the sample frequency 40 kHz, is typical of roughness noise. The power spectrum density of this signal is shown in Fig. 3. It can be observed that the energy is distributed among all frequencies. It must be noticed that the signal provided by an accelerometer has been filtered within 10 and 10 kHz by the charge amplifier. Furthermore, the signal provided by a piezo-electric accelerometer is basically proportional to the acceleration. But in this case, the charge amplifier contains an analog integration filter in order that the signal is proportional to the vibrational velocity. This time-integration imposes a slope of − 20 dB/decade which is close to the one observed in Fig. 3. From Fig. 3, it can also be observed that the number of modes as well as the modal overlap are large up to 10 kHz.

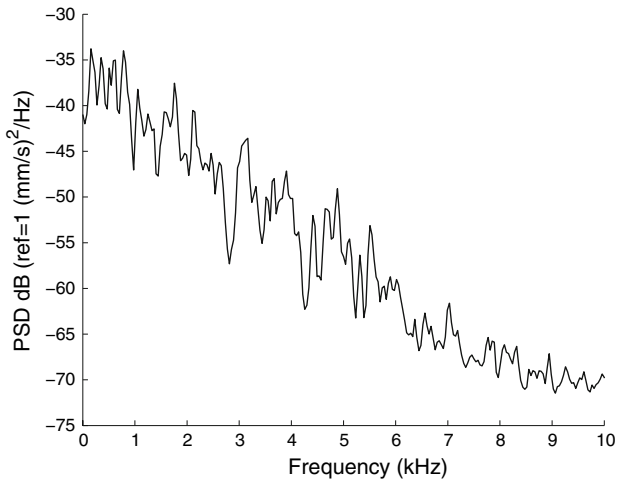

Fig. 3 Example of roughness noise. Power spectrum density: Hanning window - 1,024 lines - resolution 39 Hz - 127 averages - overlap 20%

Five experiments have been done. They combine several possibilities of plates, sliders, and surfaces.

The first four experiments have been realized with plates 200 × 300 × 2 mm (resonators A and B) and from 1 to 10 sliders. Experiment 1 is done with thick sliders, low roughness, and high damping. From this reference situation, experiment 2 investigate the influence of the internal damping $\eta\omega$, experiment 3 the influence of contact pressure (thickness of sliders), and experiment 4 the influence of the roughness of surface. The experimental conditions (resonator, slider, surface, temperature, and moisture) and results are summarized in Table 4.

In Figs. 4, 5, 6, and 7 is shown the mechanical power versus the number of sliders. The mechanical power $P = TV$ is the product of the traction force T by the sliding velocity V. In all cases, it is a linear function of the number of sliders. The mechanical power is always of order of 10 W/m^2. This is the total of mechanical power which is dissipated by all processes involved in friction, heating, wear, vibration, noise… But, the two latter phenomena contribute to a small part of the overall dissipation.

The kinematic friction coefficient μ defined as the ratio of the friction force T and the weight of sliders is also measured (Table 4). Two different values have been found corresponding to the two types of surface preparation, glass beads and corundum grits. Surfaces in experiments 1–3 are the same (glass beads) and the resulting friction coefficients have similar values $\mu = 0.24$. Experiments 1 and 3 only differ by the thickness of sliders (20 mm for experiment 1 and 10 mm for experiment 3). And a comparison of their results shows that the value of friction coefficient is not affected by the normal load. This observation is indeed in a well agreement with Amontons–Coulomb's law.

Table 4 Summary of results for the five experiments

Experiment	1	2	3	4	5
Resonator	A	B	A	A	C
Slider	Thick	Thick	Thin	Thick	Thin
Surface *Ra*	1	1	1	5	5
Temperature (°C)	22	21	21	21	22
Moisture (%)	43	38	42	35	32
P (W/m^2)	21.2	20.9	10.5	30.5	11.5
Friction coefficient μ	0.24	0.24	0.25	0.38	0.26 – 0.34
W (μJ/m^2)	3.3	33.2	1.8	50.3	2.2–25.4
λ (dB/decade)	4.4	1.7	4.8	4.5	6.7–2.2

P, mechanical power per unit area to pull the sliders; W, mean vibrational energy density; λ mean slope of the vibrational energy versus number of sliders

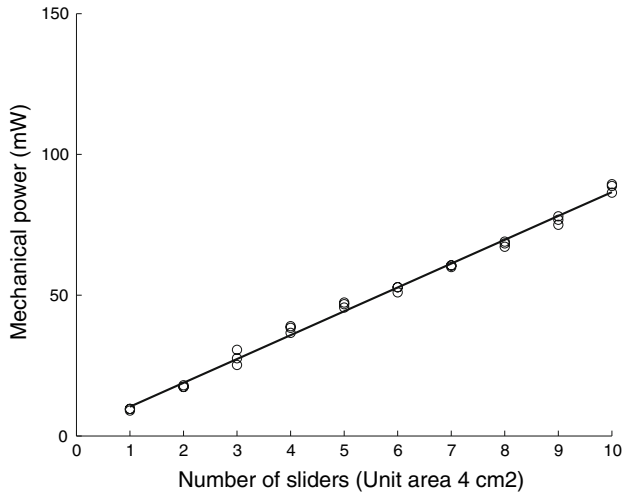

Fig. 4 Experiment 1: Mechanical power versus number of sliders. Plate 200 × 300 × 2 mm, high damping ($T_r = 0.4$ s), thick sliders 20 × 20 × 20 mm, low roughness $Ra = 1$ μm. ○, measurement; –, linear regression

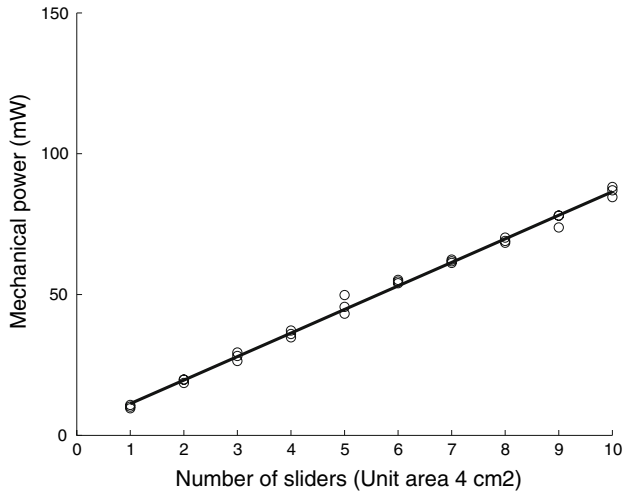

Fig. 5 Experiment 2: Mechanical power versus number of sliders. Plate 200 × 300 × 2 mm, low damping ($T_r = 21$ s), thick sliders 20 × 20 × 20 mm, low roughness $Ra = 1$ μm. ○, measurement; –, linear regression

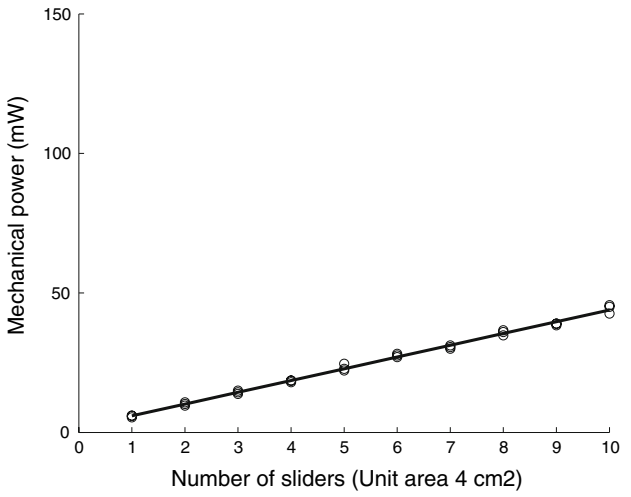

Fig. 6 Experiment 3: Mechanical power versus number of sliders. Plate 200 × 300 × 2 mm, high damping ($T_r = 0.4$ s), thin sliders 20 × 20 × 10 mm, low roughness $Ra = 1$ μm. ○, measurement; –, linear regression

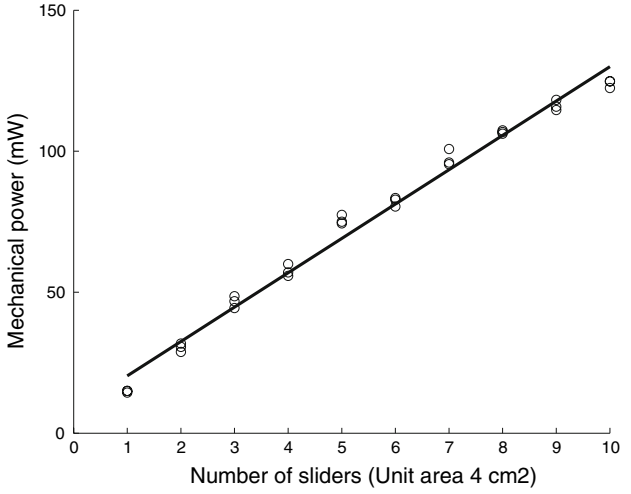

Fig. 7 Experiment 4: Mechanical power versus number of sliders. Plate 200 × 300 × 2 mm, high damping ($T_r = 0.4$ s), thick sliders 20 × 20 × 20 mm, high roughness $Ra = 5$ μm. ○, measurement; –, linear regression

Furthermore, comparison of experiments 1 and 2 which only differ by their vibrational levels ($W = 3$ μJ/m^2 for experiment 1 and $W = 33$ μJ/m^2 for experiment 2), shows that the value of friction coefficient is not affected by the vibration. This result observed in this experiment, is sometimes discussed at the atomic scale in the literature [20]. On the other hand, surfaces in experiments 4–5 are prepared by blasting corundum grits. Values of friction coefficient are also of same order for both experiments (about $\mu = 0.3$), although some variations have been observed in experiment 5. But there is a difference between friction coefficients of experiments 1–3 (glass beads) and experiments 4–5 (corundum grits), the latter being larger than the former. The blasting of corundum grits ($Ra = 5$ μm) therefore results in a greater friction coefficient than the blasting of glass beads ($Ra = 1$ μm), that is these experiments are located in the increasing part of the roughness–friction law. This dependence of the friction coefficient with roughness has been highlighted many times in the literature and the origin of the phenomenon can understood in both elastic and plastic regimes [21].

In Figs. 8, 9, 10, and 11 is shown the RMS-vibrational velocity versus the number of sliders. The number of sliders ranges from 1 to 10. In these figures, the solid line is a linear regression between $\log_{10}v$ and $\log_{10}n$. The slope λ in dB/decade is defined by,

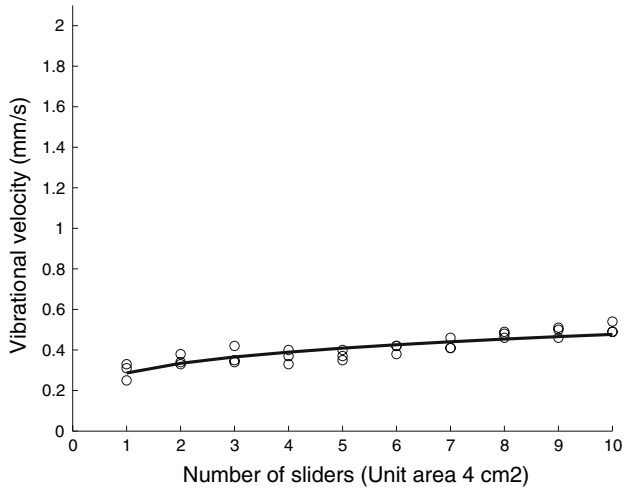

Fig. 8 Experiment 1: RMS-vibrational velocity versus number of sliders. Plate 200 × 300 × 2 mm, high damping ($T_r = 0.4$ s), thick sliders 20 × 20 × 20 mm, low roughness $Ra = 1$ μm. ○, measurement; –, linear regression in log–log plot

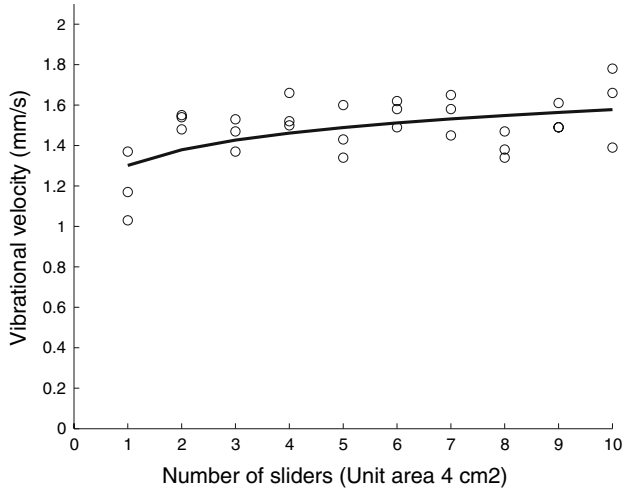

Fig. 9 Experiment 2: RMS-vibrational velocity versus number of sliders. Plate 200 × 300 × 2 mm, low damping ($T_r = 21$ s), thick sliders 20 × 20 × 20 mm, low roughness $Ra = 1$ μm. ○, measurement; –, linear regression in log–log plot

$$\lambda = 20\frac{\partial \log_{10} v}{\partial \log_{10} n} \tag{7}$$

A curve with a constant slope λ reads,

$$P_a \propto v^2 \propto n^{\lambda/10} \propto S^{\lambda/10} \tag{8}$$

In can be observed in experiments 1–4 that the slope λ varies from 1.7 to 4.8 dB/decade. A light slope means that the friction sound does not vary significantly with the number of sliders (and therefore the nominal contact area S). But a strong slope rather means that the sound level has a strong dependence with the number of sliders. The maximum of slope is 10 dB/decade for which the sound power is proportional to the number of sliders (and therefore the nominal contact area S). But, from these experiments, it can be concluded that lower slopes are possible.

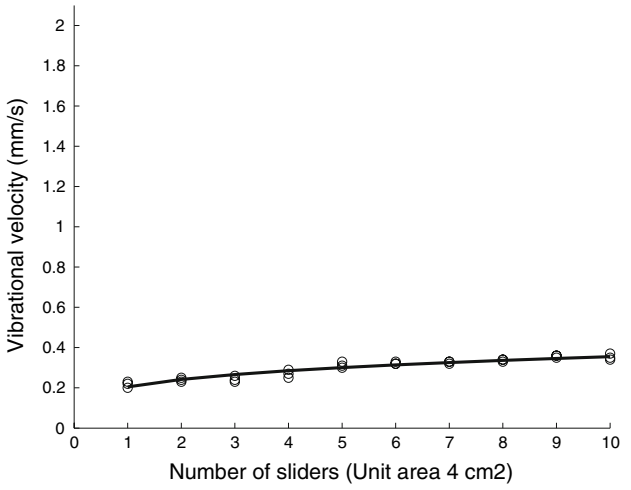

Fig. 10 Experiment 3: RMS-vibrational velocity versus number of sliders. Plate 200 × 300 × 2 mm, high damping ($T_r = 0.4$ s), thin sliders 20 × 20 × 10 mm, low roughness $Ra = 1$ μm. ○, measurement; –, linear regression in log–log plot

If experiment 1 (thick slider, low roughness, and high damping) is taken as a reference, the initial slope is 4.4 dB/decade. From experiment 2 (thick slider, low roughness, and low damping) a decrease of the internal damping leads to an increase of the vibrational level. This can be easily understood with a power balance,

$$P_i = \eta\omega \int mv^2 dA \tag{9}$$

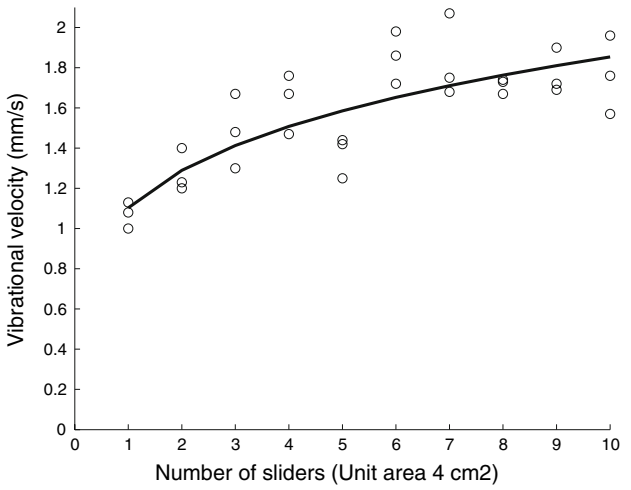

Fig. 11 Experiment 4: RMS-vibrational velocity versus number of sliders. Experiment 4: Plate 200 × 300 × 2 mm, high damping ($T_r = 0.4$ s), thick sliders 20 × 20 × 20 mm, high roughness $Ra = 5$ μm. ○, measurement; –, linear regression in log–log plot

where P_i is the vibrational power injected into the resonator by interaction processes in the contact and the right-hand side is the power being dissipated by internal processes. The term P_i has the same value in experiments 1 and 2 since surfaces and sliders are the same. Therefore a low value of $\eta\omega$ (experiment 2) results in a high value of v^2 (this is something rather well-known). But, in the same time, a decrease of internal damping leads to a decrease of the slope λ. That is, a reverberant resonator naturally trends to a regime where the vibrational level is constant, i.e., does not depend on the number of sliders. In opposition, a highly damped resonator rather behaves in a regime where the vibrational energy is proportional to the number of sliders.

From experiment 3 (thin slider, low roughness, high damping), where the thickness of sliders has been divided by 2, the vibrational energy is also divided by 2. This is in good agreement with the fact that the mechanical power and therefore the radiated acoustic power, have been divided 2. But the trend on the slope λ is not so clear. The variation of slopes between experiment 1 (thick sliders $\lambda = 4.8$) and experiment 3 (thin sliders $\lambda = 4.4$) is not significant and it can not be concluded that the thickness of sliders modifies the regime of slope.

From experiment 4 (thick slider, high roughness, and high damping) where the roughness of surface is now high, the same conclusions hold. The vibrational level is significantly increased but the slope λ is not significantly modified.

From experiments 1–4, it has been observed that various conditions of internal damping lead to various regimes of vibration versus number of sliders (slope λ). But it is also interesting to check if these regimes can be observed on a single system. This is the purpose of experiment 5. The resonator is plate C (300 × 450 × 2 mm) with a damping layer. But now, the number of sliders ranges from 1 to 80. The proportionality of the mechanical power with the number of sliders indeed remains valid as shown in Fig. 12. But the variations of the vibrational level versus the number of sliders shown in Fig. 13, now clearly have several slopes. The dependence is firstly strong $\lambda = 6.7$ dB/decade close to the perfect additive regime (10 dB/decade). And when the number of sliders is large, the dependence almost vanishes $\lambda = 2.2$ close to the perfect constant regime (0 dB/decade).

Thus, from experiments 1 to 4, a power law,

$$P_a \propto S^{\lambda/10} \tag{10}$$

applies but with various values of the exponent λ located between two extreme regimes. First of all the linear regime is,

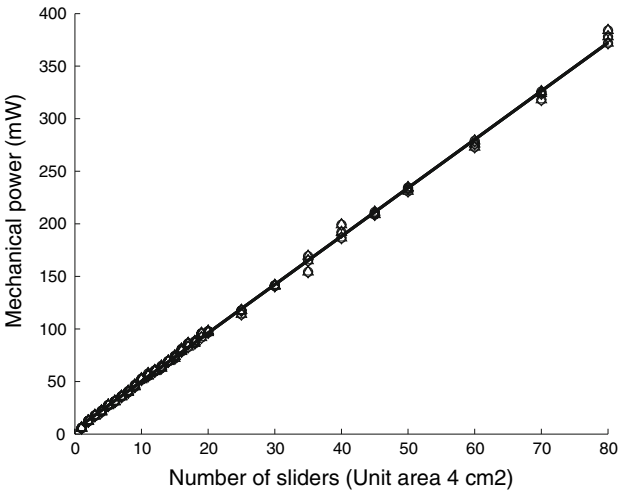

Fig. 12 Experiment 5: Mechanical power versus number of sliders. Plate 300 × 450 × 2, sliders 20 × 20 × 10 mm, roughness $Ra = 5$ μm and high damping $T_r = 0.3$ s. ○, accelerometer 1; ⋄, accelerometer 2; Δ, accelerometer 3; –, linear regression

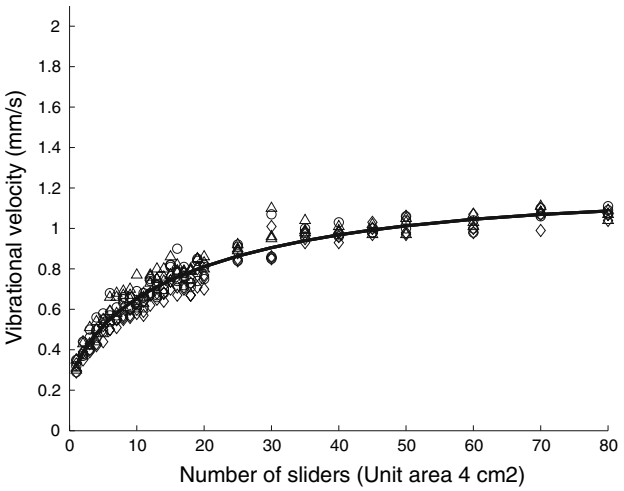

Fig. 13 Experiment 5: RMS-vibrational velocity versus number of sliders. Plate 300 × 450 × 2, sliders 20 × 20 × 10 mm, roughness $Ra = 5$ μm and high damping $T_r = 0.3$ s. ○, accelerometer 1; ⋄, accelerometer 2; Δ, accelerometer 3;–, polynomial interpolation of degree 3 in log-log plot

$$P_a \propto S \tag{11}$$

that is a slope $\lambda = 10$ dB/decade. Secondly, the constant regime is,

$$P_a \propto 1 \tag{12}$$

that is a slope $\lambda = 0$ dB/decade. But in experiment 5 where the number of sliders varies over two decades, it is clear that the slope is no longer constant. A more suitable relationship is rather,

$$P_a \propto S^{\lambda(S)/10} \tag{13}$$

where $\lambda(S)$ is a decreasing function of the variable S varying within the limits $\lambda = 10$ dB/decade and $\lambda = 0$ dB/decade.

5 Conclusion

The dependence of friction noise with nominal contact area $S = nS_0$ where S_0 is the apparent contact area of a single slider, is not a simple power law $P_a \propto S^{\lambda/10}$ where λ is the slope in dB/decade. Two extreme regimes are possible. In the linear regime, the radiated acoustic power which is proportional to the vibrational energy, is in turn proportional to the number of sources n leading to $\lambda = 10$. Although this regime has not been reached in these experiments, the maximum of $\lambda = 6.7$ has been observed. In opposition, in the constant regime, the radiated acoustic power does not depend on the number of sources n. The minimum value of $\lambda = 1.7$ has been observed.

The actual systems behave between these two limit regimes. And the main conclusion of this study is that, the most important is the internal damping of the resonator, the most linear is the regime.

The second conclusion is that the slope is not constant even for a single system. In other words, it means that a power law $P_a \propto S^{\lambda/10}$ cannot be valid since the coefficient λ would depend on S! For small contact area, the system behaves in the linear regime and for large contact area, the constant regime applies.

Acknowledgments The authors gratefully acknowledge the Angence Nationale de la Recherche (ANR), France for the financial support of this study with the contract DYVIn.

References

1. Akay, A.: Acoustics of friction. J. Acoust. Soc. Am. **111**, 1525–1548 (2002)
2. Nakano, K.: Two dimensionless parameters controlling the occurrence of stick-slip motion in a 1-DOF system with Coulomb friction. Tribol. Lett. **24**, 91–98 (2006)
3. Anand, A., Soom, A.: Roughness-induced transient loading at a sliding contact during start-up. Trans. ASME J. Trib. **106**(91), 49–53 (1984)
4. Soom A., Chen, J.: Simulation of random contact vibrations at a hertzian contact during steady sliding. Trans. ASME J. Tribol. Technol. **108**, 123–127 (1986)
5. Hess, D.P., Soom, A.: Angular and normal motions at planar contacts during sliding with friction. Trans. ASME J. Tribol. **114**(3), 567–578 (1992)
6. Perret-Liaudet, J., Rigaud, E.: Response of an impacting Hertzian contact to an order-2 subharmonic excitation: theory and experiments. J. Sound Vib. **296**, 319–333 (2006)
7. Othman, M.O., Elkholy, A.H.: Surface roughness measurement using dry friction noise. Exp. Mech. **47**, 309–312 (1990)
8. Othman, M.O., Elkholy, A.H., Seireg, A.A.: Experimental investigation of frictional noise and surface-roughness characteristics. Exp. Mech. **47**, 328–331 (1990)
9. Yokoi M., Nakai, M.: A fundamental study on frictional noise. Bull. JSME **25**(203), 827–933 (1982)
10. Kato, K.: The roughness effect on the frequency of frictional sound. In: 11th nordic symposium on tribology Nordtrib 2004 conference, 1–5 June 2004, Hurtigruten, Norway (2004)
11. Stoimenov, B., Maruyama, S., Adashi, K., Kato, K.: The roughness effect on the frequency of frictional sound. Tribol. Int. **40**, 659–664 (2007)
12. Ben Abdelounis, H., Le Bot, A., Perret-Liaudet, J., Zahouani, H.: An experimental study on roughness noise of dry rough flat surfaces. Wear (available online, 2009)
13. Mourier, L., Mazuer, D., Lubrecht, A. A., Donet, C.: Transient increase of film thickness in micro-textured EHL contacts. Tribol. Int. **39**, 1745–1756 (2006)
14. Deleau, F., Mazuyer, D., Koenen, A.: Sliding friction at elastomer/glass contact: influence of the wetting conditions and instability analysis. Tribol. Int. **42**, 149–159 (2009)
15. Crighton, D. G.: The 1988 Rayleigh medel lecture: fluid loading—the interaction between sound and vibration. J. Sound Vib. **133**, 1–27 (1989)
16. Le Bot, A.: Derivation of statistical energy analysis from radiative exchanges, J. Sound Vib. **300**, 763–779 (2006)
17. Le Bot, A., Cotoni, V.: Validity diagrams of statistical energy analysis. J. Sound Vib. (accepted for publication, 2010)
18. Polack, J.D.: Modifying the chambers to play billiards, or the foundations of reverberation theory. Acustica **76**, 257–270 (1992)
19. Le Bot, A.: A functional equation for the specular refeltion of rays. J. Acoust. Soc. Am. **112**, 1276–1287 (2002)
20. Jeon, S., Thundat, T., Braiman, Y.: Effect of normal vibration on friction in the atomic force microscopy experiment. Appl. Phys. Lett. **88**, 214102 (2006)
21. Ford, I.: Roughness effect on friction for multi-asperity contact between surfaces. J. Phys. D: Appl. Phys. **26**, 2219–2225 (1993)